Synthesis and DNA-binding properties of water-soluble cationic pyropheophorbides derived from chlorophyll *a*/*b*†

Hidetoshi Taima, Naoki Yoshioka and Hidenari Inoue*

Received 5th November 2008, Accepted 16th December 2008
First published as an Advance Article on the web 30th January 2009
DOI: 10.1039/b819700h

A series of mono-, di-, tetra- and hexacationic esters of pyropheophorbide *a*/*b* have been designed and synthesized to explore the intercalation of their phorbine ring between the base pairs of double-helical DNA and the influence of their peripheral substituents on the DNA interactions. Mono-(**1**), di-(**2**, **3**) and tetra-(**4**, **5**) cationic pyropheophorbides are soluble as an oligomeric aggregate in HEPES buffer, but hexa-(**6**) cationic pyropheophorbide is soluble as a monomer at lower concentrations. The interaction of these cationic pyropheophorbide derivatives with DNA has been investigated by DNA unwinding assay, fluorescence energy transfer, and measurements of the melting temperature of the double-helical DNA and visible absorption spectra. Dicationic **2** and **3** bind outside the double-helical DNA without and/or with self-aggregation and with self-aggregation, respectively, because they cannot intercalate between the base-pairs due to their aggregation. On the other hand, tetracationic **4** and **5** and hexacationic **6** intercalate between the base pairs of the double-helical DNA. The binding mode of the cationic pyropheophorbides *a*/*b* is strongly dependent on the number and position of the cationic peripheral substituents of the pyropheophorbides.

Introduction

Over the past two decades there has been considerable interest in small molecule DNA intercalators because of their therapeutic use for cancer and genetic diseases. In particular, a wide range of intercalative cationic porphyrins has been intensively studied as a potential chemical probe for the DNA structure,[1,2] an artificial photonuclease,[3] an inhibitor of human telomerase[4] and a photosensitizer for photodynamic therapy (PDT).[5,6] A number of cationic porphyrins has been designed and synthesized to study their interaction with DNA because the DNA binding properties are expected to be influenced by the molecular structure of the porphyrins.[7,8] Based on the studies of the porphyrin–DNA interaction, three major binding modes have been proposed for the DNA binding of cationic porphyrins: intercalation, outside groove binding and outside binding with self-stacking in which porphyrins are stacked along the DNA helix.[2,3,7] The DNA binding modes of cationic porphyrins depend on the structural properties, *e.g.*, the kind and thickness of the metalloporphyrins due to the presence or absence of an axial ligand of the central metal[9] and the structure of the peripheral substituents[8,10,11] of the porphyrin ring (Fig. 1). The DNA interactions of corrole,[12] sapphyrin,[13] texaphyrin,[14] N-confused porphyrin[15] and some chlorophyll derivatives[16–18] have also been reported. These reports have received much attention because the DNA interaction, particularly in the case of intercalation, is expected to be influenced by the change in the π conjugated system of the core aromatic ring. Therefore, corrole, sapphyrin, texaphyrin, N-confused porphyrin and chlorophyll derivatives are also interesting as new DNA probes since their absorption spectra are quite different from those of porphyrins.

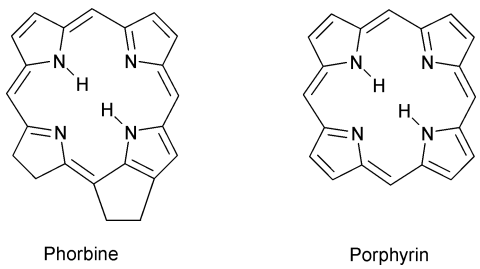

Fig. 1 Structure of phorbine and porphyrin.

In view of their application to the next generation of photonucleases or photosensitizers, the chlorophyll derivatives could be more promising because they have more intense absorption bands at the longer wavelengths than the porphyrins.[6] For *in vivo* use, photoactivation at a red-shifted wavelength is preferable since the tissue transmittance of light increases at wavelengths longer than 650 nm and the light is not absorbed by hemoglobin.[6,19] Therefore, the pyropheophorbide *a*/*b* derivatives with a phorbine ring (Fig. 2), *e.g.*, pheophorbide *a*[17] and the cationic derivatives of pyropheophorbide *a*[18] have been synthesized as new DNA binders in the previous studies. However, the pyropheophorbides, which intercalate between the base pairs of the double-helical DNA, have not been synthesized. Their interaction with DNA in a buffer solution has not been studied in detail since almost all of the pyropheophorbide derivatives so far synthesized are hardly soluble in water and present as stable aggregates.

3-14-1 Hiyoshi, Kohoku-ku, Yokohama, 223-8522, Japan. E-mail: inoue@applc.keio.ac.jp; Fax: +81 45-566-1551; Tel: +81-45-566-1555

† Electronic supplementary information (ESI) available: Experimental procedures for the synthesis of the pyropheophorbide derivatives; CD spectra of cationic pyropheophorbides (**2**–**6**); UV–vis absorption spectral changes of **2**–**6** upon the increasing addition of CT-DNA; typical melting curves of CT-DNA in the absence and presence of **6**. See DOI: 10.1039/b819700h

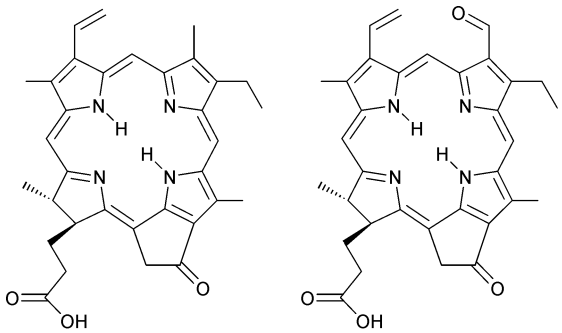

Fig. 2 Structure of pyropheophorbide *a*/*b* derived from chlorophyll *a*/*b*.

In the present work, a series of mono-, di-, tetra- and hexacationic esters of pyropheophorbides *a*/*b* (**1–6**) (Scheme 1) have been designed and synthesized. The introduction of more than two cationic peripheral substituents to the parent phorbine ring is expected to be useful for preventing the aggregation of the phorbine ring and increasing the affinity of the phorbine ring for DNA. The interaction of cationic pyropheophorbides **2–6** with the double-helical DNA has been studied by DNA unwinding assay, fluorescence energy transfer, melting temperature of the double-helical DNA and UV–vis spectroscopy. In addition, it has been elucidated whether the phorbine ring can intercalate between the base pairs of double-helical DNA and how the interaction of the cationic pyropheophorbides with DNA depends on the number and position of the cationic peripheral substituents.

Results and discussion

Synthesis of pyropheophorbide derivatives and their solution characteristics

The esterification of pyropheophorbide *a* was first attempted by the oxalyl chloride method[20] *via* the acid chloride as an intermediate. However, it was unsuccessful due to the degradation of pyropheophorbide *a*. Since the acid anhydride of pheophorbide *a* was already synthesized by a previously reported method,[21] the acid anhydride of pyropheophorbide *a* was quantitatively obtained using an excess of pivaloyl chloride in tetrahydrofuran containing pyridine, and then converted into the dimethylaminoester by excess 2-dimethylaminoethanol under heated conditions (45 °C, overnight) in high yield (about 92%). In contrast, the acid anhydride of pyropheophorbides hardly reacted with the bulky 1,1-bis(dimethylaminomethyl)-2-ethanol even under heated conditions (45 °C). In the presence of 4-dimethylaminopyridine as a catalyst,[22] it reacted with 1,1-bis(dimethylaminomethyl)-2-ethanol to give its ester derivative at room temperature. The 1,1-bis(dimethylaminomethyl)-2-ethyl-esters of pyropheophorbide *b* were synthesized by using (benzotriazol-1-yloxy)tris(dimethylamino)phosphonium hexafluorophosphate (BOP) reagent. The addition of excess BOP reagent led to the high yield of the condensation reaction between pyropheophorbide *b* and the alcohol. For example, tris[1,1-bis(dimethylaminomethyl)-2-ethyl]ester of pyropheophorbide *b* was synthesized in relatively high yield (about 72%) using about 2.7 times the molar equivalent of BOP reagent with respect to the carboxyl groups, though the desired compound with tertiary amines was partly lost because of washing with an acidic buffer solution to remove the excess BOP reagent and the byproduct derived from the BOP reagent. Thus, pivaloyl chloride is a good reagent for esterification based on the condensation yield. Otherwise, the BOP reagent, of which the intermediate is more reactive than the acid anhydride, is the best when a bulky alcohol is used. The esters of pyropheophorbide were easily converted to the corresponding cationic ammonium esters **1–6** by iodomethane.

Cationic pyropheophorbides **2–6** could be directly dissolved in 2-[4-(2-hydroxyethyl)-1-piperazinyl] ethanesulfonic acid (HEPES) buffer (5 mM, pH 7.0, 25 °C), but monocationic **1** precipitated when the solution of **1** was allowed to stand for a few hours. The molar extinction coefficients (ε) of **2–6** in HEPES buffer and dimethylsulfoxide (DMSO) are listed for the Soret band in Table 1, and the typical circular dichroism (CD) spectra of **2–6** in HEPES buffer are shown in Fig. S1 in the ESI.† The characteristic broad and blue-shifted absorption bands with a relatively small value of ε, and the typical conservative CD patterns in the Soret region[23] have revealed that **2–5** are soluble as oligomeric aggregates in HEPES buffer. The cationic pyropheophorbides that have few bulky cationic substituents are likely to aggregate due to an intermolecular π–π interaction especially on the ring II position.[24] On the other hand, the ε value at the Soret band of hexacationic **6** is reasonable as an ester derivative of pyropheophorbide *b*[21] or pheophorbide *b*[25] in the organic solvent and the vis spectral absorbance of **6** obeys the Lambert–Beer law up to 2×10^{-5} M. In addition, the ε value of hexacationic **6** in DMSO is as large as that in HEPES buffer, and the Soret band of **6** in DMSO is scarcely shifted from that in HEPES buffer (Table 1). The CD spectrum of **6** in HEPES buffer with a positive signal in the Soret region is very similar to that in DMSO (Fig. S1 in the ESI†). These vis and CD spectroscopic features of hexacationic **6** have demonstrated that **6** is soluble in HEPES buffer as a monomer, differently from the already synthesized pyropheophorbide derivatives, and that three cationic substituents, especially at the 2- and 3-positions, cause strong electrostatic and steric repulsion to prevent hexacationic **6** from aggregating.

Binding modes evidenced by fluorescence energy transfer and unwinding assay

Energy transfer from the DNA to the DNA binder (porphyrin or ethidium bromide, etc.) has been considered as evidence for intercalation. For intercalation, it can occur only if a close contact exists between the base pairs and the DNA binder,[26,27] but in the case of the outside binding mode, it does not usually occur.[26,27] The fluorescence emission of DNA-bound or free pyropheophorbides

Table 1 Molar extinction coefficients (ε) of cationic pyropheophorbides in 5 mM HEPES and DMSO at 25 °C

	HEPES		DMSO	
Compound	λ/nm	$\varepsilon \times 10^4$/M^{-1}cm^{-1}	λ/nm	$\varepsilon \times 10^4$/M^{-1}cm^{-1}
2	385.0	6.65	416.0	12.5
3	381.0	4.50	415.0	12.1
4	383.0, 414.0	6.96, 6.34	385, 419	6.93, 9.58
5	429.0	9.65	434.0	14.8
6	442.0	14.6	443.0	14.6

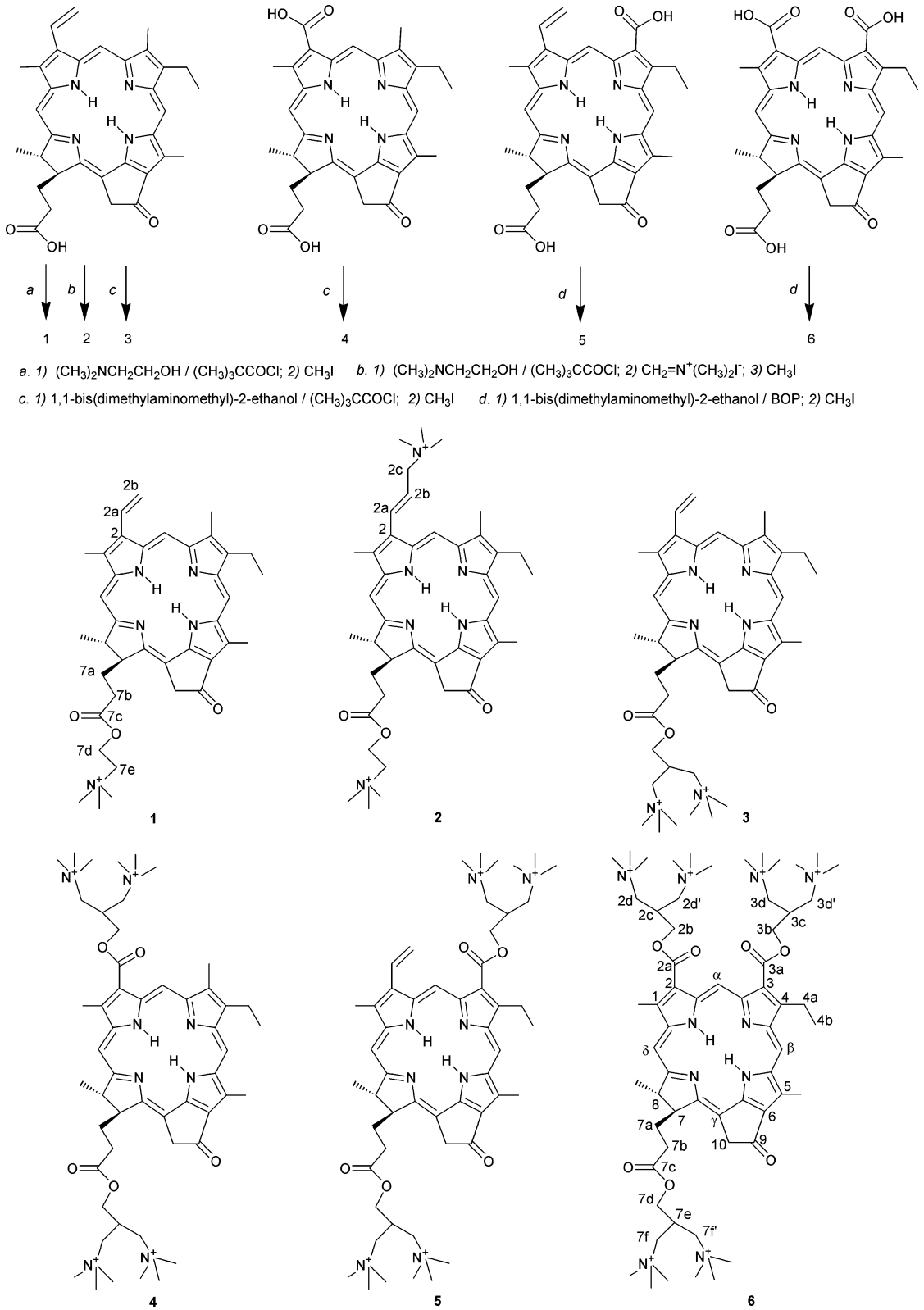

Scheme 1 Synthetic route to cationic pyropheophorbides **1–6**. The detailed route is shown in Schemes S1–S5 in the ESI.†

2–6 was measured at R = 0.1, where R is the molar ratio of [pyropheophorbide] to [DNA in base pairs], by excitation in the wavelength range of 250 to 310 nm. The fluorescence quantum yield ($Q_{\lambda 1}/Q_{\lambda 2}$) was calculated by eqn 1(see Experimental section) and is shown as a function of the excitation wavelength (Fig. 3). Pyropheophorbides **4–6** exhibited a high quantum

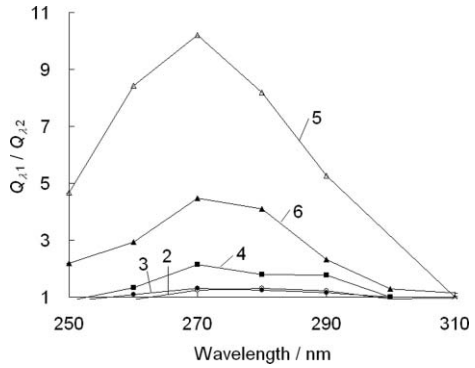

Fig. 3 Variation in the fluorescence quantum yield of cationic pyropheophorbides (**2–6**) in the presence of CT-DNA as a function of excitation wavelength.

yield at 270 nm. The fluorescence emission maxima of **5** and **6** are at 666 and 686.5 nm, respectively, but the emission maximum of **4** is at a longer wavelength of 712 nm. In contrast, pyropheophorbides **2** and **3** did not show any significant increase in the fluorescence quantum yield between 250 and 320 nm. Thus, pyropheophorbides **4–6** intercalate between the base pairs of the double-helical DNA, while **2** and **3** bind outside the double-helical DNA.

The DNA unwinding assay is also a crucial means of assessing the ability of small molecule DNA binders to intercalate between the double-helical DNA. In the present study, plasmid DNA was relaxed by incubation with topoisomerase I, followed by further treatment with the DNA binders. After the deactivation of topoisomerase I and the removal of the DNA binders, the plasmid DNA was analyzed by agarose gel electrophoresis.[28] The experimental results obtained for **2–6** by the DNA unwinding assay are shown in Fig. 4. As can be seen from Fig. 4, the plasmid DNA (pBR322 DNA, Form I) was fully relaxed to Form II by topoisomerase I (lane 2). The relaxed Form II DNA was fully unwound by virtue of the interaction of **4–6**, while it was not unwound to Form I by **2** or **3**. Therefore, the results of the DNA unwinding assay have clearly shown that **4–6** intercalate between the base pairs of the double-helical DNA, but **2** and **3** bind outside the double-helical DNA.

The helix unwinding angle can be calculated from the electrophoretic mobility because it is reflected in the number of superhelical turns in plasmid DNA.[29] The unwinding angle (θ) of **6** was estimated by the following method. The centre of the Boltzmann distribution of the topoisomers, which corresponds to the writhing number (τ), was read and the change induced by the addition of the DNA binders ($\Delta\tau$) was calculated. The molar ratio of the DNA binder to the plasmid DNA was then used to calculate the induced unwinding per added molecule of DNA binder. For example, the $\Delta\tau$ value, *i.e.*, the change in the centre of the topoisomer distribution between lanes 3 and 5 (Fig. 4E) is 5. The difference in the concentration of the DNA binder between lanes 3 and 5 is 0.42 μM, and the DNA concentration is 4.9×10^{-3} μM. The Δm value, *i.e.*, the increase in the number of DNA-binder molecules bound to one pBR322 molecule is 85.6 (from lanes 3 to 5) because the equilibrium constant (K_{app}) of **6** is sufficiently large (3.8×10^5 M^{-1}, in Table 3) and the increase in the concentration of the DNA-bound **6** from lane 3 to lane 5 can be equal to that in the concentration of **6** (0.416 μM). Thus, the θ of **6** is calculated to be 21° according to eqn 2 (see Experimental section). When similar calculations were repeated between lanes 3 and 4, and lanes 4 and 5, the θ of **6** was determined to be 22 ± 2°. The θ of **4** and **5** were determined in a similar way, and are listed in Table 2. The unwinding angle induced by the DNA intercalation increases in the order **6** > **5** > **4**. The unwinding angle of cationic pyropheophorbide *b* derivatives **5** and **6** is about two-fold that of the cationic pyropheophorbide *a* derivative **4**. In the case of **5** and **6**, a relatively large distortion from the ideal B-form DNA is required for intercalation of these molecules with a bulky cationic substituent at the 3-position. Indeed, the θ value is significantly influenced by the molecular structure and thus the position of the cationic substituent. Interestingly, the θ value of tetracationic **5** is larger than that of 5,10,15,20-tetrakis(*N*-methylpyridinium-4-yl)porphyrin (TMPyP) (19°)[30] or tetracationic chlorin e_6 (16 ± 2°).[16] The low symmetry in the phorbine ring compared with the

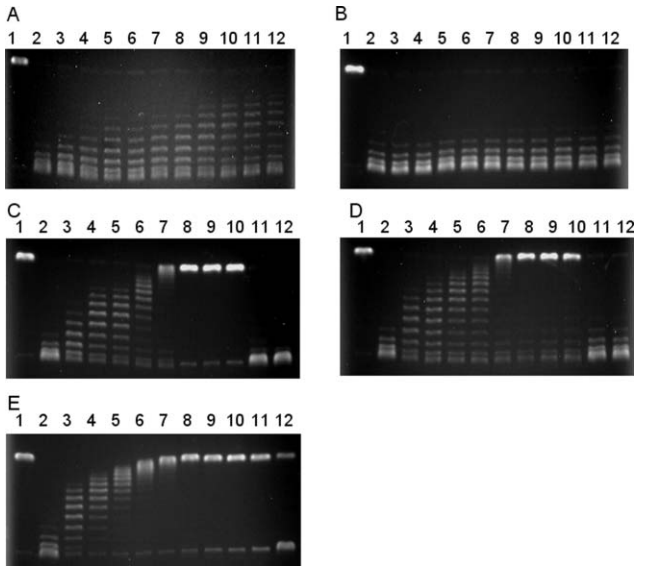

Fig. 4 Agarose gel electrophoresis of pBR322 DNA relaxed by topoisomerase I in the presence of **2** (panel A), **3** (panel B), **4** (panel C), **5** (panel D) and **6** (panel E). Lane 1: pBR322 DNA (Form I), Lane 2–12: pBR322 DNA (Form I, 0.5 μg in 35 μL) treated by 10 units of topoisomerase I in the presence of **2**, **3**, **4**, **5** or **6** at the following concentrations (R = [pyropheophorbide]/$[DNA]_{base\ pairs}$), respectively. Panel A–B; 0(0), 0.25(0.012), 0.45(0.021), 0.67(0.031), 0.87(0.041), 1.1(0.052), 1.9(0.090), 2.5(0.12), 3.7(0.18), 6.0(0.28), 7.9 μM (0.37). Panel C; 0(0), 0.41(0.019), 0.74(0.035), 1.1(0.051), 1.4(0.067), 1.8(0.085), 3.1(0.15), 4.1(0.19), 6.1(0.29), 9.7(0.46), 1.3 μM (0.61). Panel D; 0(0), 5.4(0.026), 7.6(0.036), 1.0(0.048), 1.5(0.072), 1.7(0.080), 4.8(0.23), 6.3(0.30), 9.5(0.45), 1.5(0.72), 2.0 μM (0.96). Panel E; 0(0), 0.25(0.012), 0.45(0.021), 0.67(0.031), 0.87(0.041), 1.1(0.052), 1.4(0.067), 1.9(0.090), 2.5(0.12), 3.7(0.18) and 6.0 μM (0.28).

Table 2 Unwinding angle of pBR322 DNA induced by interaction with cationic pyropheophorbides

Compound	Unwinding angle/°
2	–
3	–
4	10 ± 1
5	20 ± 1
6	22 ± 2

chlorin or porphyrin ring must contribute to the relatively large value of θ observed upon intercalation of the pyropheophorbides. In addition, it can be stated that the binding mode of the cationic pyropheophorbides to DNA is also strongly influenced by the cationic peripheral substituents on the phorbine ring.

Binding mechanism characterized by absorption spectroscopy

The changes in the vis spectra of **6** upon the addition of calf thymus DNA (CT-DNA) are shown in Fig. 5 and S2 in the ESI.† At R ≥ 0.33, where cationic **6** is electrically in excess compared with anionic CT-DNA, substantial hypochromism with an isosbestic point was found for the Soret and Q bands. In contrast, significant hyperchromism with a new isosbestic point and a large red shift was observed at R ≤ 0.33. Based on the results of the spectrophotometric titration, the interaction of **2–6** with CT-DNA proceeds in two steps (Fig. 5 and S2-S6 in ESI†). In the first step, the absorption spectra of **2–6** exhibit hypochromicity with a slight shift in the Soret and Q bands as the R values decrease to the electroneutrality point. The vis spectral changes are very fast and reach an equilibrium within a few minutes after mixing **2–6** with CT-DNA in the buffer solution. These features of the vis spectral changes suggest that the first step of the binding process is an electrostatic interaction of cationic **2–6** with the phosphate anion site of CT-DNA. In the second step, the negative charges on the phosphate anion site of CT-DNA are stoichiometrically in excess at R ≤ 1 for **2** and **3**, R ≤ 0.50 for **4** and **5** or R ≤ 0.33 for **6**. The tangling of CT-DNA electrically neutralized by cationic **2–6** will be relaxed to retain the solubility of CT-DNA in the buffer solution. As a result, the vis spectra of **2** and **4–6** show a shift in the Soret and Q bands as the R values decrease in the second step. In contrast, pyropheophorbide **3** hardly shows a shift in the Soret and Q bands as the R values decrease in the second step. The vis-spectral changes of **2–6** in the second step are relatively slow compared with those in the first step, and the hyperchromicity and shift of the Soret and Q bands are not very significant anymore and are almost independent of the decrease in the R values at R = 0.03. In other words, the second step is almost completed at R = 0.03. From the spectral features, it is suggested that **2–6** are relocated to another site on the double-helical DNA.

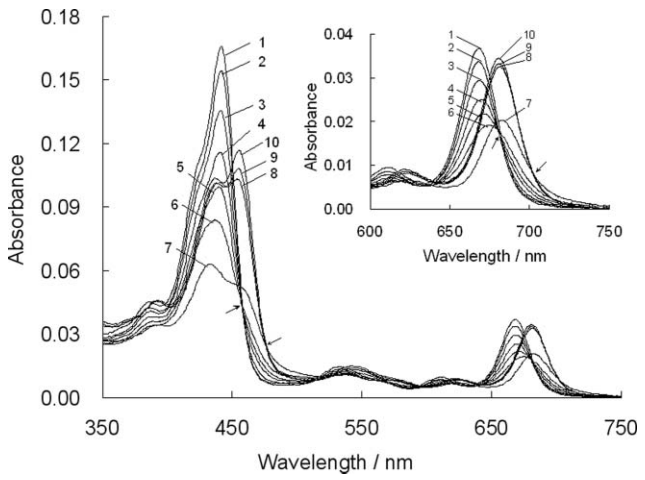

Fig. 5 Visible absorption spectral change of **6** in the presence of CT-DNA in 5 mM HEPES at 25 °C. The number attached to the absorption spectra corresponds to decreasing R values; number 1(R = ∞), 2(10), 3(2.0), 4(1.0), 5(0.7), 6(0.5), 7(0.3), 8(0.1), 9(0.07), 10(0.03). Complete data on **2–5** are provided as Fig. S2 and S3 in the ESI.†

In the second step, new broad, red-shifted and complicated absorption spectra were observed for **2** in the Soret region and accompanied by substantial hyperchromicity upon the addition of CT-DNA. In addition, the absorption bands of **2** in the second step appeared at longer wavelengths (411–425 nm) than those in DMSO (416.5 nm). These results have suggested that in the second step **2** is bound outside the double-helical DNA without and/or with self-aggregation *i.e.*, self-stacking in which **2** is stacked along the DNA helix. In the second step, the absorption bands of **3** in the Soret and Q band region exhibited no shift, but substantial hyperchromicity upon the addition of CT-DNA. These results have shown that **3** is relocated at R ≤ 1 and bound outside the double-helical DNA with self-aggregation in a manner similar to that in the DNA-free solution as the molecules of **3** are overlapping by optimizing the van der Waals contact with each other.[31] Thus, dicationic pyropheophorbides **2** and **3** cannot intercalate between the base pairs of CT-DNA because they have few cationic substituents. Since dicationic **2** and **3** give rise to weaker electrostatic and steric repulsion at the electroneutrality point of R than tetracationic and hexacationic intercalators **4–6**, the aggregation of **2** and **3** is hardly broken and prevents their intercalation between the base pairs of CT-DNA.

In the second step, **4–6** are intercalated between the base pairs of the double-helical DNA based on the results of the DNA unwinding assay and fluorescence energy transfer. Interestingly, all the absorption maxima of **4–6** in the Q band region are red-shifted and show hyperchromicity with a new isosbestic point in the second step. On the other hand, the vis spectra of **4** and **5** in the Soret band region are complicated and have two new peaks. At least one is red-shifted from the monomeric original absorption peak in DMSO (for **4** and **5**) and the other is blue-shifted, although upon intercalation between the base pairs of CT-DNA, the Soret band of the porphyrins is usually red-shifted (Δλ ≥ 15 nm) from the monomeric original Soret band.[1,2] These characteristic spectral changes may be explained as follows. The symmetry of the phorbine ring is lower than that of the porphyrin ring, and thus the phorbine ring is distorted by intercalating between the base pairs of the double-helical DNA and interacting with the base pairs *via* π–π interaction, so that the degeneracy of the HOMO, LUMO, or both is unfolded to shift the energy level and the absorption band.

The apparent equilibrium constants (K_{app}) of **4–6** in the second step were calculated in the range of R = 0.1–0.03 by eqn 3 (see Experimental section) (Fig. S7-S9 in ESI†) and are listed in Table 3. According to the definition of K_{app} (see Experimental Section),

Table 3 Apparent equilibrium constants (K_{app}) between cationic pyropheophorbides and CT-DNA in the second step in 5 mM HEPES

Compound	$K_{app}{}^{a} \times 10^4/M^{-1}$
2	–
3	–
4	2.0
5	6.7
6	38

[a] at R = 0.1–0.03.

the large K_{app} means that the pyropheophorbides tend to easily move from the first binding position, where all the quaternary nitrogens of the pyropheophorbides stoichiometrically bind to all the phosphate anion sites of CT-DNA by electrostatic force, to the second binding site where the pyropheophorbides intercalate between the base pairs of the double-helical DNA. The K_{app} of **5** is larger than that of **4**, suggesting that the cationic substituents attached to the 2- or 3-position of the phorbine ring influence the K_{app} values to some extent. The K_{app} of **6** is larger than those of **4** or **5**. Therefore, the K_{app} also depends on the number of cationic substituents when the kind of cationic substituents attached to the pyropheophorbide is the same. This is probably because pyropheophorbides with more cationic substituents give rise to stronger electrostatic repulsions among the pyropheophorbide molecules at the first binding position.

Binding strength assessed by measurements of melting temperature

The thermal denaturation of the double-helical DNA from double-stranded to single-stranded DNA manifests as hyperchromism in the UV absorption of the DNA base pairs at 260 nm. The melting temperature (T_m) of DNA is sensitive to its double-strand stability and the DNA binding of small molecules alters the T_m depending on the strength of the interactions.[32] Upon the binding of small molecules to calf thymus DNA (CT-DNA), the T_m of the B-form DNA should increase as compared with that of free CT-DNA. In addition, the increase in T_m becomes larger as small molecules are more strongly bound to DNA.[33] Therefore, the T_m can be used as an indicator of the binding properties of DNA binders and their binding strength. Upon adding cationic pyropheophorbides **2–6** to the DNA solution, the profile of the melting curve did not drastically change although the T_m was higher than that of free CT-DNA (Fig. S10 in ESI†). The increase in melting temperature (ΔT_m), *i.e.*, the difference in the melting temperatures in the absence and presence of cationic pyropheophorbides is plotted against the R value (Fig. 6). The increasing addition of the cationic pyropheophorbides **2–6** to the buffer solution of CT-DNA raises the T_m to some extent, indicating that the double-helical CT-DNA is stabilized by the binding of **2–6**. When the ΔT_m for these cationic pyropheophorbides are compared with each other at the larger R values, *e.g.*, R = 0.2, the larger the number of positive charges of the pyropheophorbides, the larger the ΔT_m is, although the ΔT_m for dicationic **3** at smaller R values, *e.g.*, R = 0.1, is larger than that for tetracationic **5**. This is because the concentration effect of outside binders on the rising

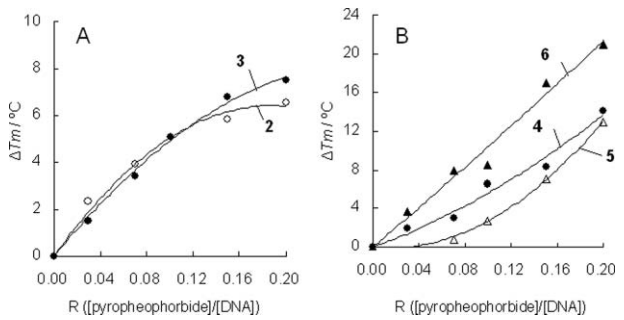

Fig. 6 Plots of the increase in melting temperature (ΔT_m) vs. the molar ratio of pyropheophorbides **2–6**to CT-DNA in base pairs (R).

of T_m is different from that of intercalators. Interestingly, the ΔT_m for outside binders **2** and **3** logarithmically increases with the R value in the range of R = 0–0.2. It is well known that the ΔT_m logarithmically increases with the concentration of sodium ions in buffer solution.[34] Therefore, outside binders **2** and **3** might behave like sodium ions in buffer solution with regard to the stabilization of the double-helical CT-DNA by electrostatic interaction between the cation sites of pyropheophorbides and the anion sites of the double-helical DNA. On the other hand, the ΔT_m for intercalators **4–6** does not logarithmically increase with the R value, suggesting that the cationic intercalator is taken up into a site of the base pairs in the double-helical DNA to interact with the nucleic acid bases through the π–π interaction.

Experimental

Fluorescence Energy Transfer

The fluorescence measurements were performed by a JASCO FP-777W fluorescence spectrophotometer using a 10 mm quartz cell at 25 °C. The fluorescence spectra were recorded with the following instrument parameter settings: bandwidth = 3 nm (excitation) and 5 nm (emission), response time = 0.5 s, step resolution = 0.5 nm, and scan speed = 500 nm/min. When porphyrins and other dyes intercalate between the base pairs of the double-helical DNA, energy transfer from the excited nucleic acid bases to the porphyrins or other dyes takes place.[10,27] The contact energy transfer from the nucleic acid bases to the bound pyropheophorbides was measured in 5 mM HEPES buffer at 25 °C by fluorescence emission as well as UV–vis absorption in the presence of CT-DNA as a function of excitation wavelength. A solution of cationic pyropheophorbides in HEPES buffer was added to that of CT-DNA in HEPES buffer to adjust the R value to 0.1. The solution mixture was stirred for 30 min, and the emission and UV–vis spectra were measured at 25 °C. In all the emission spectra, the concentration of CT-DNA was 3.23×10^{-6} M at R = 0.1, at which the absorbance at the excitation wavelength was kept below 0.05 so that reabsorption effects would be negligible. All the UV–vis spectra were measured in the concentration range in which the Lambert–Beer law could be applied to both pyropheophorbides and CT-DNA. All the absorbance values of the cationic pyropheophorbides and CT-DNA in 5 mM HEPES at 25 °C were lower than 1.0 in a quartz cell. Correction at each point was calculated by the comparison of UV–vis and fluorescence emission spectra.[10,27] The ratio of the quantum yield of the bound pyropheophorbide with excitation in the UV spectral region of the nucleic acid ($Q_{\lambda 1}$) to that with excitation at 300 nm (for **3** and **4**), 310 nm (for **5**) or 320 nm (for **2** and **6**) of the bound pyropheophorbide ($Q_{\lambda 2}$) was calculated using eqn 1.[10,27]

$$\frac{Q_{\lambda 1}}{Q_{\lambda 2}} = \left(\frac{I_{\lambda 1} \times \varepsilon_{\lambda 2}}{I_{\lambda 2} \times \varepsilon_{\lambda 1}}\right)_b \left(\frac{I_{\lambda 2} \times \varepsilon_{\lambda 1}}{I_{\lambda 1} \times \varepsilon_{\lambda 2}}\right)_f \quad (1)$$

where I and ε are the measured fluorescence intensities and molar extinction coefficients of the free (f) and bound (b) pyropheophorbides (at R = 0.1), respectively. The wavelength 300, 310 or 320 nm was chosen as the normalization wavelength for each cationic pyropheophorbide because of the negligible absorption of nucleic acids in this region.

DNA unwinding assay

Typically pBR322 DNA (closed circular Form I, 0.5 μg in 33 μL (pH 7.9) of 26.7 mM tris(hydroxymethyl)aminomethane (Tris), 1.4 mM EDTA, 7.5 mM NaCl, 1.2 mM dithiothreitol (DTT) and 1.1% glycerol) was incubated with wheat germ topoisomerase I (10 units) at 37 °C for 60 min to afford a relaxed plasmid DNA (open circular Form II). To the relaxed plasmid DNA topoisomers (33 μL) were added specific amounts of the cationic pyropheophorbides (2.0 μL) in different concentrations. The mixtures (35 μL) were then incubated at 37 °C for 60 min. The topoisomerization was stopped with 3 μL of 10% sodium dodecyl sulfate (SDS), and extracted with TE saturated phenol (35 μL). After mixing and centrifugation, the upper aqueous phase was re-extracted with CIA (chloroform/isoamyl alcohol = 24/1, 30 μL). The above operations (after addition of the pyropheophorbides) were done in the dark to prevent exposure to light. The mixture of the upper phase (22 μL) and loading buffer (5.5 mM orange G, 30% glycerol, 5.5 μL) was subjected to 1% agarose gel. The gel was electrophoresed for 5.5 h on TAE (40 mM Tris–acetate/1 mM EDTA) buffer at 50 V (5.6 V/cm) at room temperature. After electrophoresis, the gel was stained for 30 min in ethidium bromide (1.0 μg/mL) and excess ethidium bromide was removed by standing in distilled water for 10 min. The DNA bands were detected by UV light from a transilluminator and the fluorescence emission was visualized by a CCD camera connected to a Vilber Lourmat DP-001 FDC photodocumentation system for Windows. From the electrophoresis, the DNA-unwinding angle (θ) can be calculated using eqn 2.[29]

$$\theta\,(\text{in }^\circ) = 360\,\Delta\tau/m \tag{2}$$

where $\Delta\tau$ is the change in the writhing number and m is the number of dye molecules bound to one pBR322 molecule.

Spectral measurements

All measurements, except where specifically indicated, were performed in HEPES buffer. The UV–vis absorption spectra were recorded in solution by a JASCO V-570 spectrophotometer equipped with a JASCO ETC-505T temperature controller using a 10 mm quartz cell at the spectral band pass of 1 nm with a 0.1 nm spectral resolution. The circular dichroism (CD) spectra were measured by a JASCO J-720WI spectropolarimeter using 10 mm quartz cells. The CD spectra were recorded with the following instrument parameter settings: bandwidth = 2.0 nm, response time = 2.0 s, step resolution = 0.5 nm, and scan speed = 200 nm/min between 350–500 nm. The apparent equilibrium constants (K_{app}) at R = 0.1–0.03 for the equilibrium between DNA-bound pyropheophorbide at the electroneutrality point and DNA-bound pyropheophorbide in the second step were determined by absorption spectrophotometric measurements at 25 °C. The fixed amount of HEPES buffer solution of CT-DNA (2.0 mL) in various concentrations was mixed with a specific volume of HEPES buffer solution of the pyropheophorbide to give the R value in the range of 0.1–0.03 in a quartz cell, and then the mixed solution was stirred to reach equilibrium as checked by the UV–vis spectra. The absorbance was measured at the maximum wavelength of the Q band. The apparent equilibrium constant (K_{app}) between the cationic pyropheophorbide and CT-DNA was calculated using eqn 3.[35]

$$[\text{DNA}]_{total}/(|\varepsilon_{app} - \varepsilon_1|) = \{1/(|\varepsilon_2 - \varepsilon_1|)\}[\text{DNA}]_{total} + 1/\{K_{app}(|\varepsilon_2 - \varepsilon_1|)\} \tag{3}$$

where ε_{app}, ε_1 and ε_2 correspond to A_{obsd}/[pyropheophorbide], the extinction coefficient for the pyropheophorbide in the fully bound form at the electroneutrality point (R = 0.5 for **4** and **5** and R = 0.33 for **6**) and the extinction coefficient for the pyropheophorbide in the fully bound form in the second step, respectively. Here, cationic pyropheophorbides **4–6** are considered to be present as a monomer at R ≤ 0.5 for **4** and **5** and R ≤ 0.33 for **6** because the pyropheophorbides intercalate as monomers between the base pairs of the double-helical DNA as evidenced by the unwinding angle of **4–6** calculated using eqn 1. Thus, ε_1 and ε_2 are assumed to be concerned with a monomeric species of the pyropheophorbides. In the plot of $[\text{DNA}]_{total}/(|\varepsilon_{app} - \varepsilon_1|)$ *vs.* $[\text{DNA}]_{total}$, K_{app} is given by the ratio of the slope to the intercept.[35] Unfortunately, K_{app} for **2** or **3** cannot be calculated because the aggregation number of **2** or **3** cannot be determined in the range of R = 0.1–0.03 because the cationic pyropheophorbides **2** and **3** bind outside the phosphate backbone of the DNA with self-aggregation.

Measurements of melting temperature (T_m)

The melting of polynucleotide strand from double-helical DNA manifests itself as absorption hyperchromicities in the 260 nm region. The melting temperature (T_m) is generally increased upon the addition of DNA binders. The samples were prepared according to the following procedure. The concentration of the CT-DNA solution was determined by the extinction coefficient of $\varepsilon_{260} = 1.31 \times 10^4$ M^{-1} cm^{-1} for CT-DNA.[36] A solution of CT-DNA (16–26 μM, 2.0 mL) in HEPES buffer (5 mM, pH 7.0 at 25 °C) was mixed with various amounts of the cationic pyropheophorbides at certain concentrations in HEPES buffer (pH 7.0) to give the R value of 0–0.2 in a quartz cell with a magnetic stirrer, a Teflon stopper and a 10 mm path length. The quartz cell filled with the sample solution was placed in a jacketed cell compartment regulated by a JASCO ETC-505T cell-temperature controller with heating and refrigeration capabilities. The temperature was measured using a thermister probe attached to the ETC-505T controller and inserted into the quartz cell containing the sample solution through a hole of the Teflon stopper. The absorbance of the sample solution at 260 nm was measured and taken automatically every 10 s by a JASCO V-570 or V-550 spectrophotometer equipped with the JASCO ETC-505T temperature controller while the sample solution was continuously stirred and gradually heated from 25 to 95 °C at the rate of 2 °C/min. The T_m was taken as the temperature at the maximum in the plot of absorbance *vs.* 1/temperature.[37] The increase in T_m (ΔT_m) was calculated by subtracting the T_m at R = 0 from the T_m for each R value.

Conclusions

Six cationic pyropheophorbides **1–6** have been designed and synthesized by esterification using pivaloyl chloride (**1–3**) or BOP reagent (**4–6**). Hexacationic **6** with an aromatic phorbine ring is soluble in HEPES buffer as a monomer because of the large

electrostatic repulsion and steric hindrance due to the 2- and 3-substituents. On the other hand, di-(**2**, **3**) and tetra-(**4**, **5**) cationic pyropheophorbides are soluble in HEPES buffer as an oligomeric aggregate. When the DNA is electrically in excess compared with the pyropheophorbides, dicationic **2** and **3** bind outside the double-helical DNA without and/or with self-aggregation and with self-aggregation, respectively, while tetracationic **4** and **5** and hexacationic **6** intercalate between the base pairs of the double-helical DNA. In order to synthesize DNA intercalators, it is not always necessary to design a molecule which is soluble in buffer solution as a monomer. However, it is important for the design of the cationic pyropheophorbides as DNA intercalators to introduce as many cationic and relatively bulky substituents at suitable positions as possible so that the electrostatic repulsion and steric hindrance might increase. The DNA unwinding assay and measurements of the fluorescence energy transfer, melting temperature of the double-helical DNA and vis absorption spectra have revealed that binding features such as the binding mode, DNA unwinding angle, equilibrium constant and binding strength of the cationic pyropheophorbide *a*/*b* derivatives can be controlled by the number and position of the cationic peripheral substituents.

Acknowledgements

This work was supported in part by a Grant-in-Aid for Scientific Research (No. 13554025) from the Ministry of Education, Culture, Sports, Science and Technology of the Japanese Government.

Notes and references

1 (*a*) R. F. Pasternack and E. J. Gibbs, *Met. Ions Biol. Syst.*, 1996, **33**, 367–397; (*b*) V. A. Galievsky, V. S. Chirvony, S. G. Kruglik, V. V. Ermolenkov, V. A. Orlovich, C. Otto, P. Mojzes and P.-Y. Turpin, *J. Phys. Chem.*, 1996, **100**, 12649–12659.
2 (*a*) R. J. Fiel, *J. Biomol. Struct. Dyn.*, 1989, **6**, 1259–1275; (*b*) R. F. Pasternack and E. J. Gibbs, *ACS Symp. Ser.*, 1989, **402**, 59–73.
3 (*a*) B. Armitage, *Chem. Rev*, 1998, **98**, 1171–1200; (*b*) D. S. Sigman, *Biochemistry*, 1990, **29**, 9097–9105; (*c*) S. Yellappa, J. Seetharamappa, L. M. Rogers, R. Chitta, R. P. Singhal and F. D'Souza, *Bioconjugate Chem.*, 2006, **17**, 1418–1425; (*d*) Y. Ishikawa, N. Yamakawa and T. Uno, *Bioorg. Med. Chem.*, 2007, **15**, 5230–5238.
4 (*a*) H. Mita, T. Ohyama, Y. Tanaka and Y. Yamamoto, *Biochemistry*, 2006, **45**, 6765–6772; (*b*) H. Han, D. R. Langley, A. Rangan and L. H. Hurley, *J. Am. Chem. Soc.*, 2001, **123**, 8902–8913; (*c*) T. Yamashita, T. Uno and Y. Ishikawa, *Bioorg. Med. Chem.*, 2005, **13**, 2423–2430; (*d*) C. Wei, G. Jia, J. Yuan, Z. Feng and C. Li, *Biochemistry*, 2006, **45**, 6681–6691; (*e*) D.-F. R. Shi, T. Wheelhouse, D. Sun and L. H. Hurley, *J. Med. Chem*, 2001, **44**, 4509–4523.
5 (*a*) D. Kessel, R. Luguya and M. G. Vicente, *Photochem. Photobiol.*, 2003, **78**, 431–435; (*b*) J. Moan, K. Berg, and E. Kvam, in *Photodynamic Therapy of Neoplastic Disease*, ed. D. Kessel, CRC Press, Boca Raton, 1990, vol. 1, pp. 197–209.
6 (*a*) E. S. Nyman and P. H. Hynninen, *J. Photochem. Photobiol. B: Biol.*, 2004, **73**, 1–28; (*b*) R. Bonnett, *Chem. Soc. Rev.*, 1995, **24**, 19–33.
7 L. G. Marzilli, *New. J. Chem.*, 1990, **14**, 409–420.
8 D. R. McMillin, A. H. Shelton, S. A. Bejune, P. E. Fanwick and R. K. Wall, *Coord. Chem. Rev.*, 2005, **249**, 1451–1459.
9 (*a*) R. F. Pasternack, E. J. Gibbs and J. J. Villafranca, *Biochemistry*, 1983, **22**, 2406–2414; (*b*) N. R. Barnes, A. F. Schreiner, M. G. Finnegan and M. K. Johnson, *Biospectroscopy*, 1998, **4**, 341–352; (*c*) N. R. Barnes and A. F. Schreiner, *Inorg. Chem.*, 1998, **37**, 6935–6938; (*d*) J. S. Trommel and L. G. Marzilli, *Inorg. Chem.*, 2001, **40**, 4374–4383; (*e*) J. A. Strickland, L. G. Marzilli, K. M. Gay and W. D. Wilson, *Biochemistry*, 1988, **27**, 8870–8878; (*f*) U. Sehlstedt, S. K. Kim, P. Carter, J. Goodisman, J. F. Vollano, B. Nordén and J. C. Dabrowiak, *Biochemistry*, 1994, **33**, 417–426.
10 M. A. Sari, J. P. Battioni, D. Dupré, D. Mansuy and J. B. Le Pecq, *Biochemistry*, 1990, **29**, 4205–4215.
11 (*a*) S. Wu, Z. Li, L. Ren, B. Chen, F. Liang, X. Zhou, T. Jia and X. Cao, *Bioorg. Med. Chem.*, 2006, **14**, 2956–2965; (*b*) D. H. Tjahjono, T. Akutsu, N. Yoshioka and H. Inoue, *Biochim. Biophys. Acta*, 1999, **1472**, 333–343; (*c*) K. Andrews and D. R. McMillin, *Biochemistry*, 2008, **47**, 1117–1125; (*d*) A. H. Shelton, A. Rodger and D. R. McMillin, *Biochemistry*, 2007, **46**, 9143–9154; (*e*) B. R. Munson and R. J. Fiel, *Nucleic Acids Res.*, 1992, **20**, 1315–1319.
12 Z. Gershman, I. Goldberg and Z. Gross, *Angew. Chem., Int. Ed.*, 2007, **46**, 4320–4324.
13 (*a*) B. L. Iverson, K. Shreder, V. Král and J. L. Sessler, *J. Am. Chem. Soc.*, 1993, **115**, 11022–11023; (*b*) B. L. Iverson, K. Shreder, V. Král, D. A. Smith, J. Smith and J. L. Sessler, *Pure. Appl. Chem.*, 1994, **66**, 845–850; (*c*) J. L. Sessler, P. I. Sansom, V. Král, D. O'Connor and B. L. Iverson, *J. Am. Chem. Soc.*, 1996, **118**, 12322–12330.
14 P. Kubát, K. Lang, Z. Zelinger and V. Král, *J. Inorg. Biochem.*, 2005, **99**, 1670–1675.
15 Y. Ikawa, S. Moriyama, H. Harada and H. Furuta, *Org. Biomol. Chem.*, 2008, **6**, 4157–4166.
16 H. Taima, A. Okubo, N. Yoshioka and H. Inoue, *Chem.–Eur. J.*, 2006, **12**, 6331–6340.
17 M. Kobayashi, S. Koyama, M. Nakazato, N. Miyoshi, C. Wolff, N. Daikuzono, C. Tanielian, M. Sasaki and M. Komiyama, *J. Clin. Laser Med. Surg.*, 1994, **12**, 133–138.
18 (*a*) S. Mansouri, S. Fery-Forgues, B. Meunier and N. Paillous, *J. Chem. Soc., Perkin Trans. 2*, 1996, 1649–1654; (*b*) S. Mansouri, A. Gossauer, B. Meunier and N. Paillous, *New J. Chem.*, 1994, **18**, 745–748; (*c*) C. Kanony, A.-S. Fabiano.-Tixier, J.-L. Ravanat, P. Vicendo and N. Paillous, *Photochem. Photobiol.*, 2003, **77**, 659–667.
19 S. Wan, J. A. Parrish, R. R. Anderson and M. Madden, *Photochem. Photobiol.*, 1981, **34**, 679–681.
20 H. Taima, A. Okubo, N. Yoshioka and H. Inoue, *Tetrahedron Lett.*, 2005, **46**, 4161–4164.
21 M. R. Wasielewski and W. A. Svec, *J. Org. Chem.*, 1980, **45**, 1969–1974.
22 S. Kim, J. I. Lee and Y. C. Kim, *J. Org. Chem.*, 1985, **50**, 560–565.
23 S. Yagai, T. Miyatake and H. Tamiaki, *J. Org. Chem.*, 2002, **67**, 49–58.
24 A.-S. Fabiano, D. Allouche, Y.-H. Sanejouand and N. Paillous, *Photochem. Photobiol.*, 1997, **66**, 336–345.
25 P. H. Hynninen and S. Lötjönen, *Synthesis*, 1980, 539–541.
26 (*a*) M. A. Sari, J. P. Battioni, D. Dupré, D. Mansuy and J. B. Le Pecq, *Biochemistry*, 1990, **29**, 4205–4215; (*b*) J.-B. LePecq and C. Paoletti, *J. Mol. Biol.*, 1967, **27**, 87–106.
27 S. R. Chatterjee, S. J. Shetty, T. P. A. Devasagayam and T. S. Srivastava, *J. Photochem. Photobiol. B: Biol.*, 1997, **41**, 128–135.
28 (*a*) L. M. Fisher, R. Kuroda and T. Sakai, *Biochemistry*, 1985, **24**, 3199–3207; (*b*) R. S. Coleman, R. J. Perez, C. H. Burk and A. Navarro, *J. Am. Chem. Soc.*, 2002, **124**, 13008–13017.
29 (*a*) K. Utsuno, K. Kojima, Y. Maeda and M. Tsuboi, *Chem. Pharm. Bull.*, 1998, **46**, 1667–1671; (*b*) C. Bailly, C. O'Huigin, R. Houssin, P. Colson, C. Houssier, C. Rivalle, E. Bisagni, J. P. Henichart and M. J. Waring, *Mol. Pharmacol.*, 1992, **41**, 845–855.
30 M. J. Carvlin and R. J. Fiel, *Nucleic Acids Res.*, 1983, **11**, 6121–6139.
31 K. Kano, H. Minamizono, T. Kitae and S. Negi, *J. Phys. Chem.*, 1997, **101**, 6118–6124.
32 S. Routier, V. Joanny, A. Zaparucha, H. Vezin, J.-P. Chatteau, J.-L. Bernier and C. Bailly, *J. Chem. Soc., Perkin Trans. 2*, 1998, 863–868.
33 (*a*) R. J. Fiel, J. C. Howard, E. H. Mark and N. D. Gupta, *Nucleic Acids Res.*, 1979, **6**, 3093–3118; (*b*) D. H. Tjahjono, S. Mima, T. Akutsu, N. Yoshioka and H. Inoue, *J. Inorg. Biochem.*, 2001, **85**, 219–228.
34 (*a*) F. J. Baldino, M. F. Chesselet and M. E. Lewis, *Methods Enzymol*, 1989, **168**, 761–777; (*b*) J. Marmur and P. Doty, *J. Mol. Biol.*, 1962, **5**, 109–118.
35 (*a*) A. M. Pyle, J. P. Rehmann, R. Mesoyer, C. V. Kumar, N. J. Turro and J. K. Barton, *J. Am. Chem. Soc.*, 1989, **111**, 3051–3058; (*b*) S. B. Mettath, R. Munson and R. K. Pandey, *Bioconjugate Chem.*, 1999, **10**, 94–102.
36 R. D. Wells, J. E. Larson, R. C. Grant, B. E. Shortle and C. R. Cantor, *J. Mol. Biol.*, 1970, **54**, 465–497.
37 L. Kibler-Herzog, B. Kell, G. Zon, K. Shinozuka, S. Mizan and W. D. Wilson, *Nucleic Acids Res.*, 1990, **18**, 3545–3555.